International Journal of Mechanical Engineering and Applications
2022; 10(2): 17-24
http://www.sciencepublishinggroup.com/j/ijmea
doi: 10.11648/j.ijmea.20221002.11
ISSN: 2330-023X (Print); ISSN: 2330-0248 (Online)

Verification Study of Probabilistic Fracture Mechanics Analysis Code for Reactor Pressure Vessel During Pressurized Thermal Shock

Ru-Feng Liu

Engineering Technology and Facilities Operation Division, Institute of Nuclear Energy Research, Taoyuan, Taiwan (ROC)

Email address:
lrf@iner.gov.tw

To cite this article:
Ru-Feng Liu. Verification Study of Probabilistic Fracture Mechanics Analysis Code for Reactor Pressure Vessel During Pressurized Thermal Shock. *International Journal of Mechanical Engineering and Applications*. Vol. 10, No. 2, 2022, pp. 17-24.
doi: 10.11648/j.ijmea.20221002.11

Received: March 14, 2022; **Accepted**: April 1, 2022; **Published**: April 14, 2022

Abstract: This investigation is to present a verification study of probabilistic fracture mechanics (PFM) analysis code for a reactor pressure vessel (RPV) during pressurized thermal shock (PTS). The probabilistic fracture mechanics code FAVOR, developed by Oak Ridge National Laboratory, is used to calculate the conditional probabilities of crack initiation and penetration for welds that are located in the RPV beltline region. The procedure includes deterministic analyses of the temperature and stress distributions through the vessel wall at the PTS, and probabilistic analyses on the vessel failure probability as a result of PTS transients. The RPV geometries, material properties, and properties related to embrittlement are those in taken from previous studies. Two previously suggested hypothetical transients, which may seriously affect RPV integrity, are also taken into account. To verify the results of PFM round robin analysis of RPV during PTS events, several models and Monte Carlo methods for determining PFM performance are used and they agree on the accuracy of the failure assessment is obtained. The present work can be regarded as various important factors about performing PFM that affect in evaluating the structural safety and operational stability of RPVs. The comparisons of the paper also support the finding that the FAVOR code is very practically useful in assessing failure probability.

Keywords: Pressurized Water Reactor, Reactor Pressure Vessel, Probabilistic Fracture Mechanics

1. Introduction

Pressurized thermal shock (PTS) is the most critical event in a pressurized water reactor (PWR) that challenges the structural integrity of the reactor pressure vessel (RPV). Several types of malfunction or accident can cause the vessel to fill suddenly with cool water and cause the temperature of the reactor coolant water to drop rapidly. Contact between the overcooling water and the inner surface of the vessel wall generates thermal gradients that induce stress states that vary in magnitude throughout the vessel wall. The tensile stresses through most of the thickness of the vessel wall are associated with Mode I opening driving forces on potentially present surface-breaking or embedded flaws. Owing to the reduced fracture toughness of the vessel material, the temperature drop that is associated with PTS can enable flaw propagation. The materials in the RPV beltline region are exposed to neutron radiation, and the exiting flaw may very rapidly propagate to form a through-wall crack and challenge the RPV integrity during operation of the plant.

Probabilistic fracture mechanics (PFM) was developed in the early 1980s [1] to assess structural integrity of nuclear components, and incorporated into regulations concerning PTS in the middle of that decade in the U.S. The U.S. NRC funded the Integrated Pressurized Thermal Shock (IPTS) program [2-4], which developed a comprehensive probabilistic approach to risk assessment. Current regulatory requirements are based on the resulting risk-informed probabilistic methodology. Regulatory Guide 1.154 [5] recommends the content and format of the plant-specific integrated PTS analyses to estimate the frequency of vessel failure that is caused by PTS events. Regulatory Guide 1.154 also specifies the acceptable primary PTS failure risk to be a mean frequency of less than 5×10^{-6} vessel failures per year.

To evaluate the precision of PFM tools and to improve related analyses, some round robin analysis programs [6-9] have already been developed to support internationally cooperative PFM techniques.

In this paper, overcooling problems are solved by using the Fracture Analysis of Vessels - Oak Ridge (FAVOR) computer code [10] to calculate the conditional probability of initiation (CPI) and the conditional probability of failure (CPF) of welds that are located in the RPV beltline region. Heavy Section Steel Technology (HSST) program at Oak Ridge National Laboratory (ORNL) originally developed the code [11] that represents the baseline NRC-selected PFM applications tool for re-assessing the current PTS regulations. In addition, some PFM assessments [12, 13] have also been performed to analysis the boiling water reactor (BWR) pressure vessels subjected to low temperature over-pressure (LTOP) even, which is a beyond design basis event to challenge the BWR RPV integrity. The loading conditions in the study include two previously suggested hypothetical transients. Key parameters for the PFM analyses, such as fluence level, inspection quality, copper content, initial reference temperature for nil ductility transition (RT_{NDT}) and warm pre-stressing, and flaw distribution, are considered to verify the probabilistic results. The results of a parameter sensitivity analysis indicate a reasonable agreement between the RPV failure probability assessment and the ASINCO (Asian Society for Integrity of Nuclear Components) round robin results in 2010. The main objectives of the RR analyses were to compare the results of PFM analyses by participants and codes; to evaluate the usability of the code and the effects of input parameter selections, and to spread the PFM analytical methodologies. The present work may be important to evaluating the safety of, and regulating, the RPVs of our domestic PWRs.

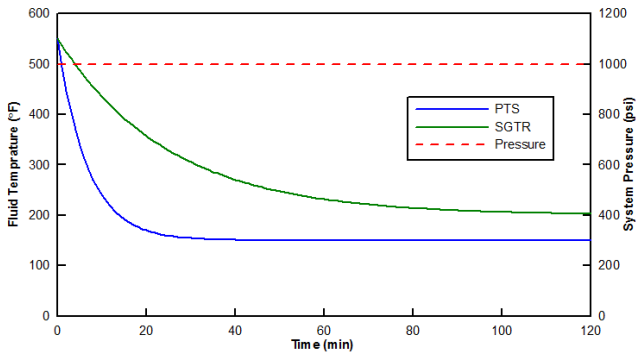

Figure 1. *Suggested hypothetical PTS and SGTR transients.*

The reactor vessel that is considered in this investigation is a typical PWR with an inner surface radius of 78.74 in. and a base metal thickness of 7.874 in. without cladding. Physical properties of the reactor vessel to perform thermal and mechanical analyses are considered those for ASTM A533B-1. The other specifications are taken from the literature [7]. As mentioned above, two hypothetical transients are considered; they are typical PTS and steam generator tube rupture (SGTR) transients. These transients are characterized by different cooling rates under a constant system pressure, as shown in Figure 1. Figure 2 displays the inspection performance. Model A is the best among those tests with providing a high inspection performance; Model C is a marginal case with relatively poor inspection performance, and Model B is the middle case that supports a moderately performing inspection.

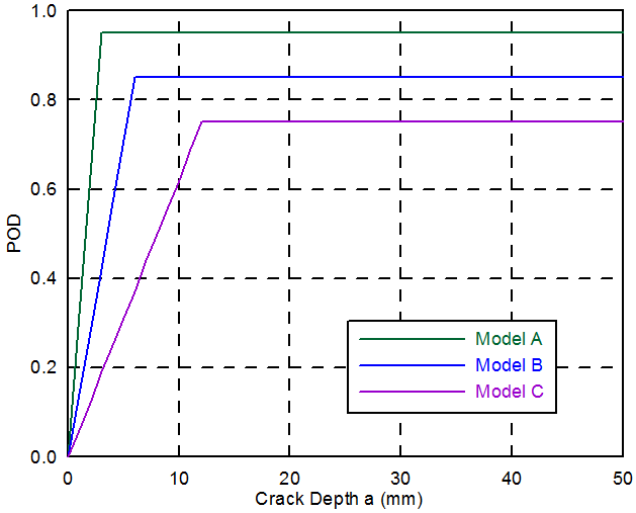

Figure 2. *Models of inspection performance.*

2. Deterministic Analyses

Theory and Implementation of Algorithms, Methods, and Correlations of the FAVOR code (e.g., ORNL/TM-2010/5) completely expounded the deterministic analyses carried out to create a loading definition for each PTS transient, including thermal analysis and stress analysis. The fundamental theories of deterministic analyses discusses in the FAVOR code user manual are briefly extracted in Section 2 of this paper.

Before probabilistic analyses are carried out, deterministic analyses of the temperature and stress distributions through the vessel wall during the transients are performed using the FAVOR code. The FAVOR code is used in both thermal and stress analyses of a one-dimensional axisymmetric model of the vessel wall. The time-dependent temperature and stress distributions through the vessel wall constitute the thermal and mechanical loading that will be applied to posited flaws. Mode I stress intensity factors are generated for a range of axially and circumferentially oriented infinite-length and finite-length (semi-elliptical) flaw geometries (flaw depths and lengths).

2.1. Thermal Analyses

The temperature time-history T(r,t) of the vessel is obtained by modeling the vessel wall as an axisymmetric one-dimensional structure whose temperature profile depends on the radial position, r, and elapsed time, t, in the transients. In the absence of internal heat generation, the transient heat conduction equation is a second-order parabolic partial differential equation:

$$\frac{\partial \mathrm{T}}{\partial \mathrm{t}} - \frac{1}{\mathrm{r}}\frac{\partial}{\partial \mathrm{r}}[\lambda(T) r \frac{\partial \mathrm{T}}{\partial \mathrm{t}}] = 0 \qquad (1)$$

where the property grouping $\lambda(T) = k(T)/\rho c_p(T)$ is the temperature-dependent thermal diffusivity of the material; ρ is the mass density; $c_p(T)$ is the temperature-dependent mass-specific heat capacity, and $k(T)$ is the temperature-dependent thermal conductivity. For Eq. (1) to be well posed, initial and boundary conditions must be applied.

Initial condition

$$T(r,0) = T_{initial} \text{ for } R_i \le r \le R_o \quad (2)$$

Boundary condition

$$q(R_i,t) = h(t)[T_\infty - T(R_i,t)] \text{ at } r = R_i \quad (3)$$

$$q(R_o,t) = 0] \text{ at } r = R_o \quad (4)$$

In Eq. (2) to Eq. (4), q is a prescribed boundary heat flux; h(t) is the time-dependent convective film coefficient; $T_\infty(t)$ is the time-dependent bulk coolant temperature, and R_i and R_o are the inner and outer radii of the vessel wall, respectively. Input data to the thermal model include the mesh definition, property data, and prescribed time-histories for h(t) and $T_\infty(t)$. In the FAVOR code, Eq. (1) to Eq. (4) can be solved using the finite element method, in which the variational formulation for the transient heat conduction equation is provided elsewhere [14].

2.2. Stress Analyses

The FAVOR code is used to carry out a displacement-based finite element analysis using a one-dimensional axisymmetric model of the vessel wall. The calculated displacements are converted into strains using strain-displacement relationships, and the associated stresses are then calculated using linear-elastic stress-strain relationships. At each time step during the transient, the structure is in a state of static equilibrium, so the load history is considered to be quasi-static. Let (u,v,w) be the radial, circumferential, and axial displacements, respectively, of a material point in a cylindrical (r,θ,z) coordinate system. The general two-dimensional axisymmetric case requires that

$$v = 0;\ \tau_{r\theta}=\tau_{\theta z}=0;\ \gamma_{r\theta}=\gamma_{\theta z}=0 \quad (5)$$

where $\tau_{r\theta}$ and $\tau_{\theta z}$ are shear stresses, $\gamma_{r\theta}$ and $\gamma_{\theta z}$ are engineering shear strains. The strain-displacement relationships in the two-dimensional case are

$$\begin{Bmatrix} \varepsilon_{rr} \\ \varepsilon_{\theta\theta} \\ \varepsilon_{zz} \\ \gamma_{rz} \end{Bmatrix} = \begin{bmatrix} \frac{\partial}{\partial r} & 0 \\ \frac{1}{r} & 0 \\ 0 & \frac{\partial}{\partial z} \\ \frac{\partial}{\partial z} & \frac{\partial}{\partial r} \end{bmatrix} \begin{Bmatrix} u \\ w \end{Bmatrix} \quad (6)$$

In the one-dimensional axisymmetric case, (r,θ,z) are principal directions, w = 0, and $\partial/\partial z = 0$, such that

$$\varepsilon_{rr} = \frac{\partial u}{\partial r};$$

$$\varepsilon_{\theta\theta} = \frac{u}{r};$$

$$\varepsilon_{zz} = \frac{\partial w}{\partial z}=0;$$

$$\gamma_{rz} = \frac{\partial u}{\partial z} + \frac{\partial w}{\partial r}=0 \quad (7)$$

In the case of a long cylinder with free ends, no axial or circumferential variation in temperature or material properties, and no radial variation in material properties, the radial and circumferential stresses in the one-dimensional axisymmetric case are calculated from the strains using

$$\sigma_{rr} = \frac{E}{(1+\upsilon)(1-2\upsilon)}[(1-\upsilon)\varepsilon_{rr} + \upsilon\varepsilon_{\theta\theta}] - \frac{\alpha E}{1-2\upsilon}(T - T_{ref});$$

$$\sigma_{\theta\theta} = \frac{E}{(1+\upsilon)(1-2\upsilon)}[(1-\upsilon)\varepsilon_{\theta\theta} + \upsilon\varepsilon_{rr}] - \frac{\alpha E}{1-2\upsilon}(T - T_{ref}) \quad (8)$$

where

σ_{rr} = radial normal stress; $\sigma_{\theta\theta}$ = hoop normal stress;
ε_{rr} = radial normal strain; $\varepsilon_{\theta\theta}$ = hoop normal strain;
T = wall temperature as a function of r;
T_{ref} = thermal stress-free reference temperature;
r = radial position in wall;
E = Young's modulus of elasticity;
υ = Poisson's ratio;
α = linear coefficient of thermal expansion.

Under generalized plane-strain conditions, the stress in the axial direction is given by

$$\sigma_{zz} = \upsilon(\sigma_{rr} + \sigma_{\theta\theta}) - \alpha E(T - T_{ref}) \quad (9)$$

In the FAVOR code, the stress time-history of a vessel is calculated using the finite element method. Eq. (8) to Eq. (9) apply to each finite element so radial variations of the material properties E, α, and ν can be considered by letting the properties vary from one element material group to another.

2.3. Linear-Elastic Fracture Mechanics

The linear-elastic stress model in the FAVOR code assumes that axial flaws are exposed to a one-dimensional axisymmetric stress field and circumferential flaws are exposed to a generalized-plane-strain stress field. These flaws are, therefore, assumed to undergo only a Mode I loading, so the principal load is applied normal to the crack plane, tending to open the crack. The plastic zone around the crack tip is also assumed to be fully contained, and the overall deformation-load response of the structure is linear. Under these high-constraint conditions, the principles of linear-elastic fracture mechanics (LEFM) are applied to calculations of driving forces of a crack. For a cracked structure under LEFM conditions, the singular stress field around the crack tip can be characterized using a single-parameter. The single-parameter model has the form

$$\sigma_{\theta\theta} = \frac{K_I}{\sqrt{2\pi \cdot r}} \text{ for axial stress;}$$

$$\sigma_{zz} = \frac{K_I}{\sqrt{2\pi \cdot r}} \text{ for hoop stress} \quad (10)$$

where r is the radial distance from the crack tip, and the crack plane is assumed to be a principal plane. The critical fracture parameter in Eq. (10) is the Mode I stress intensity factor, K_I. When the conditions for LEFM are satisfied, the problem of calculating the stress intensity factor can be formulated purely in terms of the flaw geometry and the stress distribution of the uncracked structure. The FAVOR code has an extensive stress-intensity-factor-influence coefficient (SIFIC) database for finite- and infinite-length surface flaws that somehow this ratio is implemented herein with $R_i/t = 10$ only. The HSST program of ORNL has developed a similar database for $R_i/t = 20$, which was implemented in earlier versions of the FAVOR code and can be re-installed for future releases of the code if the need arises. For inner surface breaking flaws, the stress intensity factor is calculated using the FAVOR code by a weighting-function approach that was introduced by Buckner and has since been used by other researchers, including the developers of OCA-I and OCA-P. The HSST program generated a database of SIFICs for axial infinite-length and axial semi-elliptical surface flaws along with circumferential 360-degree and circumferential semi-elliptical surface flaws. These databases have been implemented in the FAVOR code.

2.4. Results

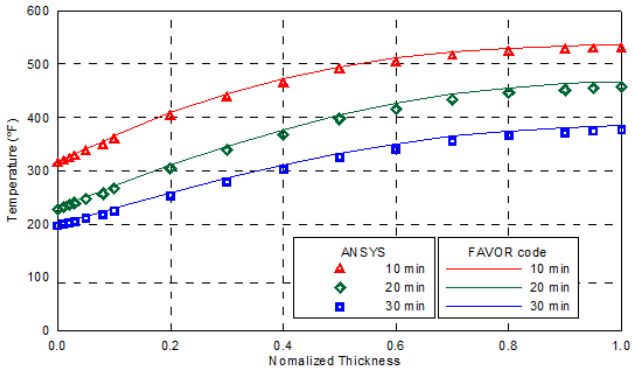

(a) Trough-wall

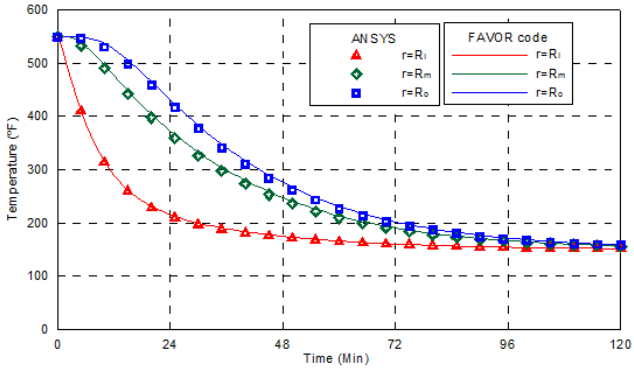

(b) Time historical

Figure 3. *Comparison of temperature distributions at PTS.*

First, the temperature distributions are calculated and analyses of the stresses that arise from these temperature distributions and internal pressure are carried out using the FAVOR code. Two hypothetical transients, PTS and SGTR, are considered in deterministic analyses for determining the temperature distributions. Figure 3 and Figure 4 show the through-wall and time historical temperature distributions at the PTS and SGTR transients that are considered in thermal analyses. For comparison, the through-wall temperature distributions at 10 min., 20 min. and 30 min. after the transients begin are displayed in these figures. Clearly, that the agreement between the temperature results obtained using the FAVOR code and those obtained using the ANSYS finite element software is fairly good. These figures indicate that the temperature decrease through the vessel wall is significantly related to the cooling rate of the reactor coolant water.

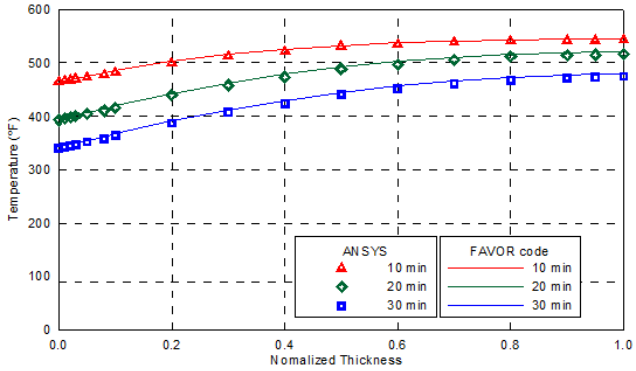

(a) Trough-wall

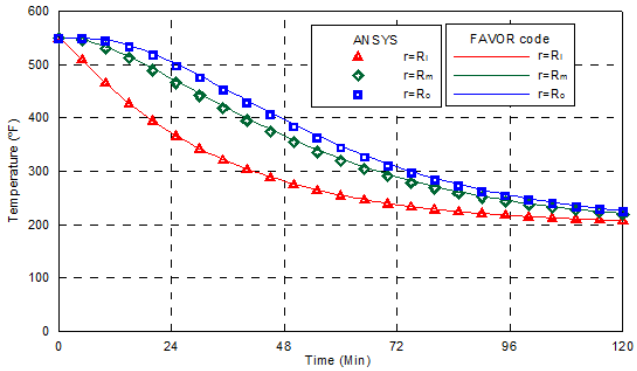

(b) Time historical

Figure 4. *Comparison of temperature distributions at SGTR.*

Figure 5 and Figure 6 show the through-wall hoop and axial stress distributions at the PTS and SGTR transients that are considered in stress analyses. The through-wall stress distributions are also displayed at 10 min., 20 min. and 30 min. after the transients start. Clearly, the stress results obtained using the FAVOR code agree fairly well with those obtained using the ANSYS finite element software. Comparing the stress distributions between the PTS and SGTR transients indicate clearly that the stresses in the vessel wall for the PTS transient are higher than those for the SGTR transient. As mentioned in relation to the thermal analyses, this difference arises from the fact that the temperature decrease in the inside surface of the wall differs owing to the difference in the cooling rate between the transients.

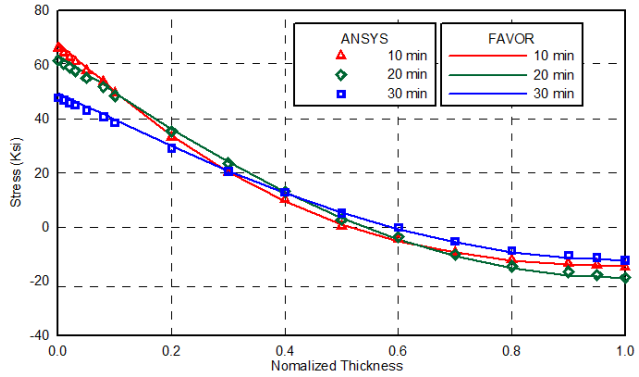

(a) Hoop stress

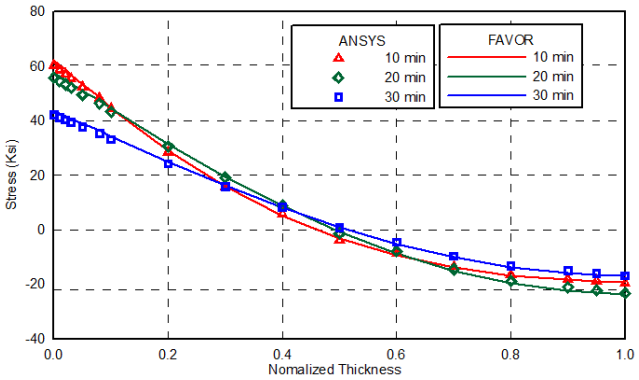

(b) Axial stress

Figure 5. *Comparison of through-wall stress distributions at PTS.*

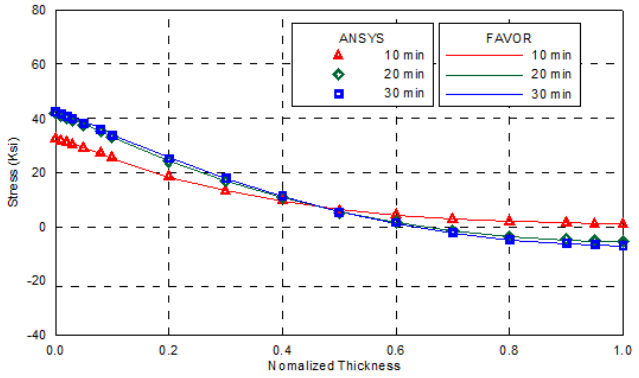

(a) Hoop stress

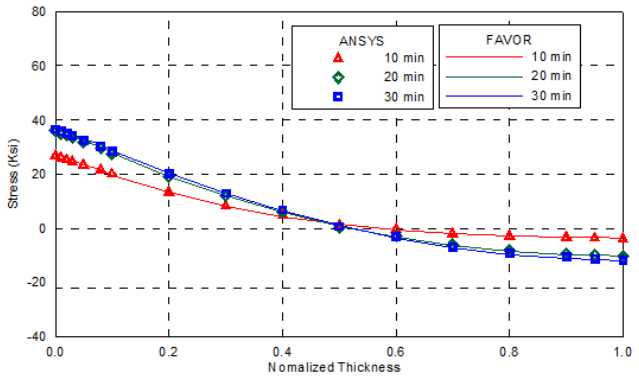

(b) Axial stress

Figure 6. *Comparison of through-wall stress distributions at SGTR.*

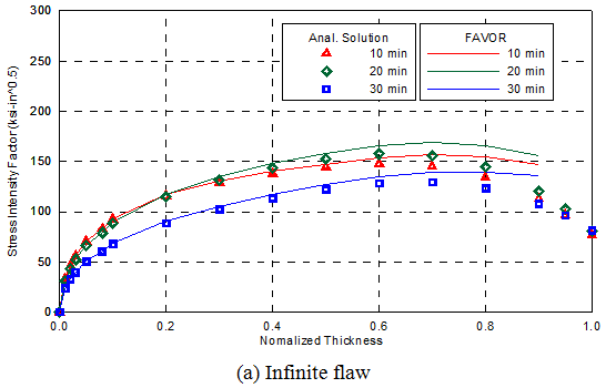

(a) Infinite flaw

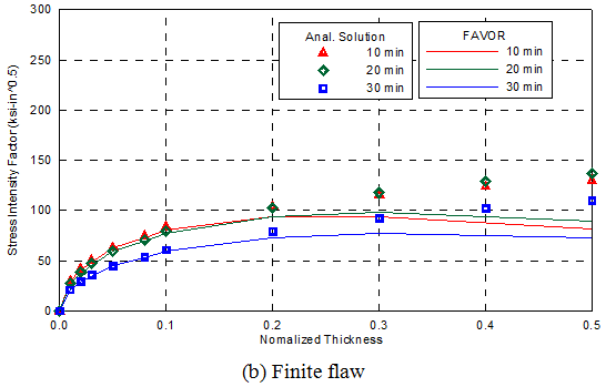

(b) Finite flaw

Figure 7. *Comparison of through-wall axial SIF distributions at PTS.*

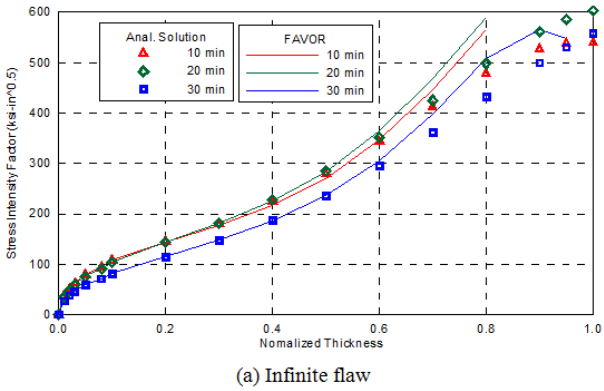

(a) Infinite flaw

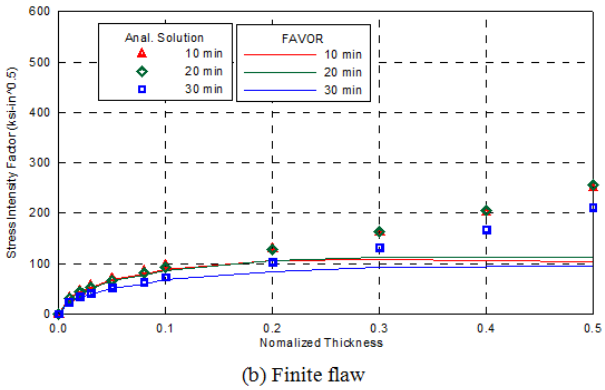

(b) Finite flaw

Figure 8. *Comparison of through-wall hoop SIF distributions at PTS.*

Stress intensity factors (SIFs), and those at the crack tip that are calculated using influence coefficient methods are shown in Figure 7 and Figure 8 for the posited flaw of an

infinite surface-breaking crack and a finite crack with an aspect ratio of 1/6 in the axial direction. The through-wall SIF distributions at 10 min., 20 min. and 30 min. after the PTS transient begin are displayed. The SIF results obtained using the FAVOR code are compared with those obtained using the Buchalet and Bamford solution [15]. From these figures, SIFs increase with wall thickness. The SIFs reach peak values around 20 min. after the transient starts. The large SIFs are caused by the large thermal stress that arises from the steep temperature gradient. The temperature distributions through the vessel wall are also used to calculate the fracture toughness. The SIF and fracture toughness are compared to determine the propagation of the crack that causes the failure of the vessel, which is used to calculate the risk of vessel failure in probabilistic analyses.

3. Probabilistic Analyses

3.1. Description of Problems

To carry out probabilistic analyses, a base problem using an SGTR transient without inspection is defined. Problem 1 concerns a PTS transient and the other settings are the same as for the base problem. Problem 2 considers the inspection performance, which is mentioned above. Problem 3 and Problem 4 are used to perform sensitivity analyses of PFM for copper content (0.1, 0.2 and 0.3 wt.%) in RPV steel and the initial RT_{NDT} (-10°C and -40°C). Problem 5 and Problem 6 can be used for other sensitivity analyses that involve warm pre-stressing (WPS) effect and flaw distribution (Marshall and fixed size).

3.2. Results

To verify PFM performance, all of the probabilistic results obtained using the FAVOR code are compared with those of the ASINCO round robin (RR) analyses that are calculated by Japanese and Korean research groups [7]. The Japanese group involved a probabilistic code PASCAL2. The Korean group used a probabilistic code VISA-II. Although CPI results are not obtained by the RR analyses, CPI and CPF results that are obtained using the FAVOR code are plotted as a function of neutron fluence in Figure 9 to Figure 14 for the various problems.

Problem 1

As shown in Figure 9, the failure probabilities at a transient increase with the neutron fluence. The probabilistic results that arise from the PTS transient are higher than those that arise from the SGTR transient by one or two orders of magnitude, depending on the fluence level. The effect of transient severity, which is the difference between the cooling rates of the PTS and SGTR transients, is clearly revealed.

Problem 2

Figure 10 displays the effect of inspection quality, and includes a no-inspection case. The failure probabilities that are caused by four flaw distributions - no inspection, and inspection models A, B, and C are obtained using the FAVOR code. The inspection quality is incorporated into the Marshall flaw distribution. The results thus obtained indicate that Marshall distributions without inspection and with Model A (very good) inspection yield the highest and lowest probabilities, respectively. The best inspection reduces the probability of failure at a transient by one order of magnitude relative to no inspection.

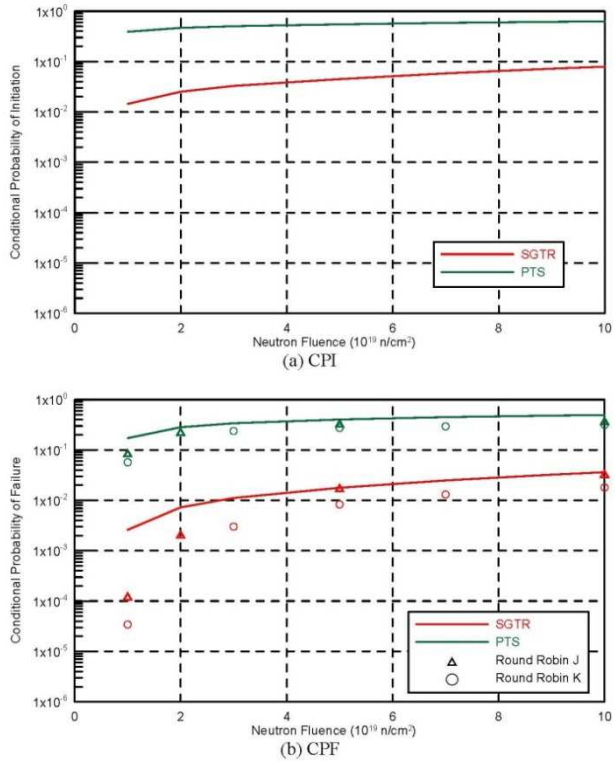

Figure 9. *Effect of transient type and fluence on the probability.*

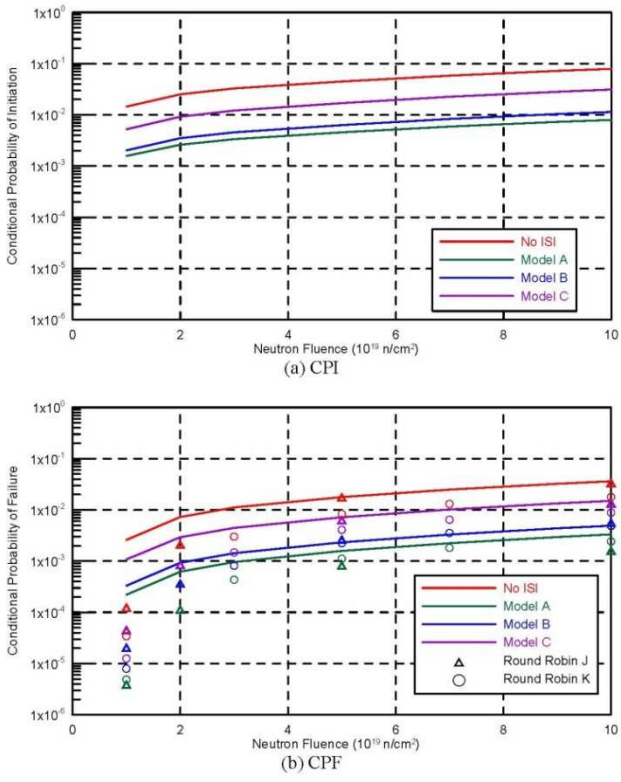

Figure 10. *Effect of inspection quality and fluence on the probability.*

Problem 3 & 4

Figure 11 and Figure 12 display the effects of copper content and initial RT_{NDT} on the probabilistic results. The failure probabilities in the problems of interest have the same effect on increase of equally increase the neutron fluence. As the copper content decreases, the failure probability falls greatly. The initial RT_{NDT} has a small effect on the probabilistic results.

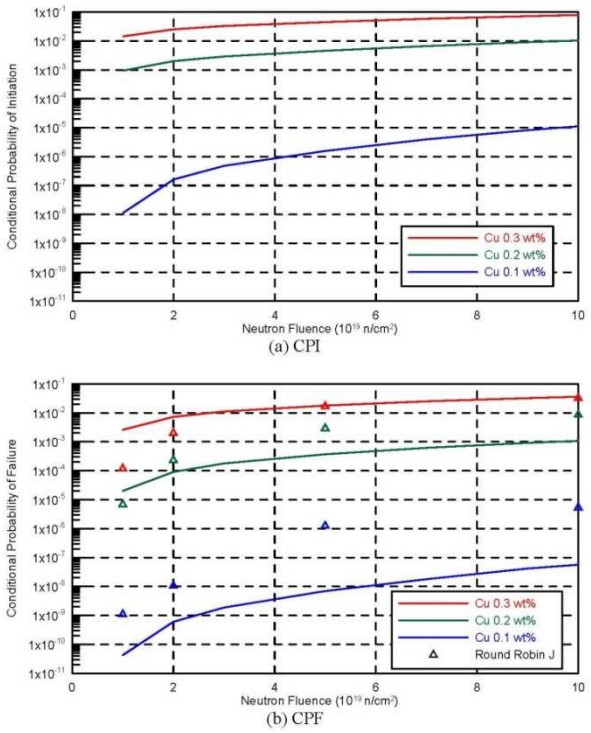

Figure 11. *Effect of copper content and fluence on the probability.*

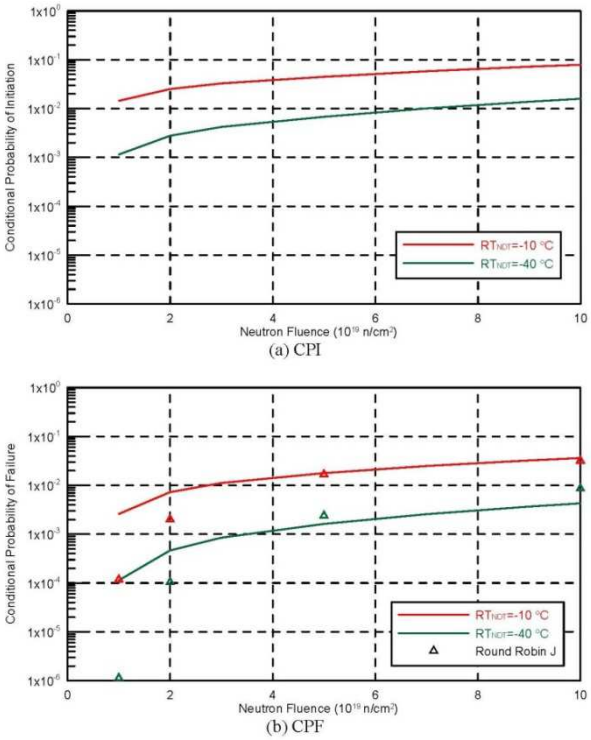

Figure 12. *Effect of RT_{NDT} and fluence on the probability.*

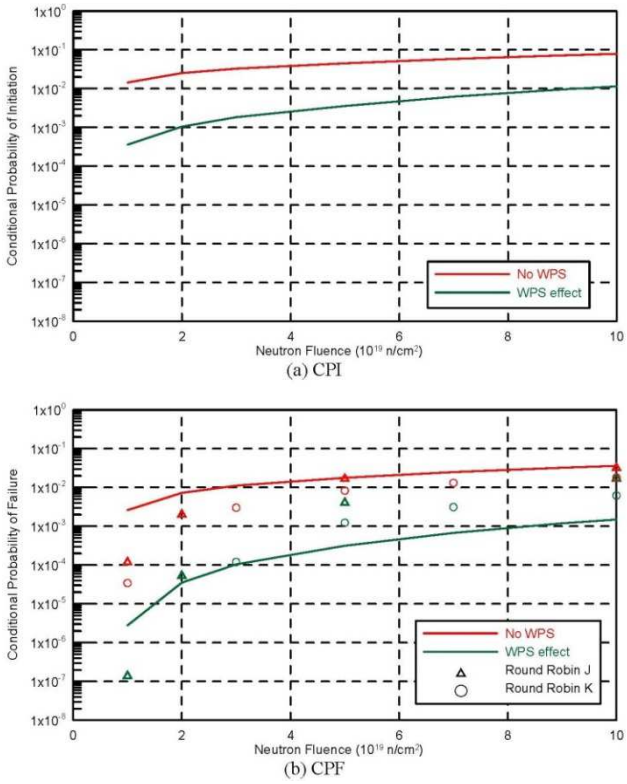

Figure 13. *Effect of warm pre-stress and fluence on the probability.*

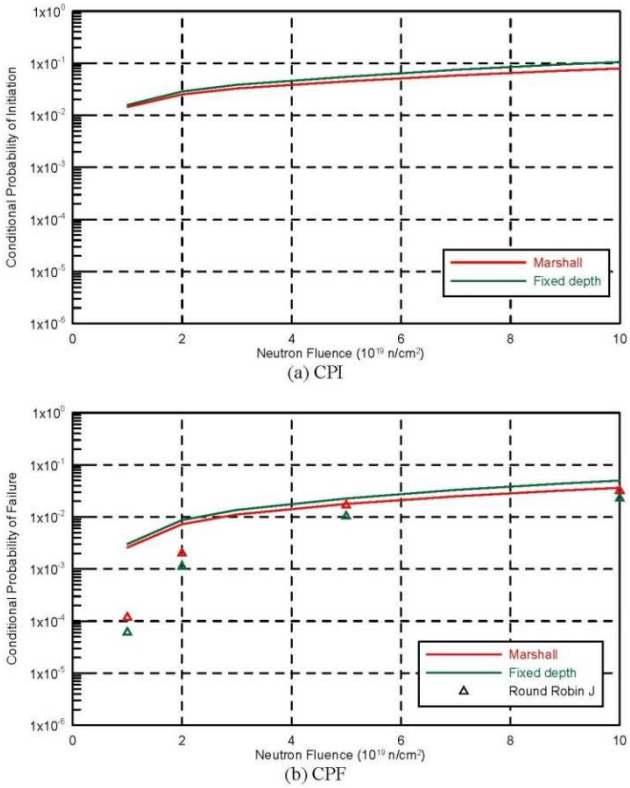

Figure 14. *Effect of flaw distribution and fluence on the probability.*

Problem 5&6

One of the items in probabilistic analyses is the WPS effect; the other is an effect of initial crack distribution. Figure 13 and Figure 14 show probabilistic results. The

WPS effect is based on the basic premise that a crack will not be initiated if the SIF is dropping over time or constant as the temperature is dropping. Consideration of the WPS effect reduces failure probabilities by one or two orders of magnitude. At low fluence, the CPF value becomes very low as a result of the WPS effect. The effect of the crack size of the Marshall distribution and a fixed size of 10 mm deep by 60 mm long gave small difference. Therefore, the Marshall distribution may correspond to such a fixed crack size.

The probabilistic results obtained using the FAVOR code are compared with those of the RR analyses. The above results indicate that the results obtained using the FAVOR code agree with the results RPV failure probability assessment that based on the ASINCO RR analyses.

4. Conclusion

PFM analyses for welds that are located in a RPV beltline region that is subjected to PTS are carried out using the FAVOR code in the study. Two hypothetical transients and several inspection models are considered to calculate failure probabilities. Results of deterministic temperature and stress analyses, LEFM analyses, and probabilistic analyses are compared. The results in this paper support the following important engineering conclusions.

1. The results of deterministic analyses of the temperature and stress in an RPV wall at the transients agree very closely.
2. Since all of the RR analyses herein used other PFM analysis tools, the results that are obtained herein using the FAVOR code agree closely with those of the RR analyses in general.
3. Some parameters, such as transient type, inspection quality, copper content and warm pre-stressing, importantly affect failure probability.

The comparisons also support the finding that the FAVOR code is very practically useful in assessing failure probability. This investigation improves our empirically based knowledge of PFM performance.

Acknowledgements

The author would like to acknowledge the financial support of Taiwan Power Company. (under grant no. 054010000101).

References

[1] 10 CFR 50.61. (1984). Fracture Toughness Requirements for Protection against Pressurized Thermal Shock Events, U.S. Nuclear Regulatory Commission.

[2] NUREG/CR-3770 (ORNL/TM-9176). (1986). Preliminary Development of an Integrated Approach to the Evaluation of Pressurized Thermal Shock as Applied to the Oconee Unit 1 Nuclear Power Plant, U.S. Nuclear Regulatory Commission.

[3] NUREG/CR-4022 (ORNL/TM-9408). (1985). Pressurized Thermal Shock Evaluation of the Calvert Cliffs Unit 1 Nuclear Power Plant, U.S. Nuclear Regulatory Commission.

[4] NUREG/CR-4183 (ORNL/TM-9567). (1985). Pressurized Thermal Shock Evaluation of the H. B. Robinson Nuclear Power Plant, U.S. Nuclear Regulatory Commission.

[5] R. G. 1.154. (1987). Format and Content of Plant-Specific Pressurized Thermal Shock Safety Analysis Reports for Pressurized Water Reactors, U.S. Nuclear Regulatory Commission, U.S. Nuclear Regulatory Commission.

[6] NEA/CSNI/R (2007) 18. (2008). Proceedings of the CSNI Workshop on Structural Reliability Evaluation and Mechanical Probabilistic Approaches of NPP Components, Nuclear Energy Agency.

[7] Kanto, Y., Jhung, M.-J., Ting, K., & Yoshimura S. (2010). Summary of international PFM round robin analyses among asian countries on reactor pressure vessel integrity during pressurized thermal shock, The 8th International Workshop on the Integrity of Nuclear Components, Hyogo (Japan).

[8] Soneda, N., Onchi, T. (1996). Benchmarking studies of probabilistic fracture mechanics analysis code, PROFMAC-11, for assessing pressurized thermal shock events of reactor pressure vessel integrity issues. J. Nucl. Sci. Technol 33 (1): 87-98. doi: 10.1080/18811248.1996.9731866.

[9] Jhung, M. J., Kim, S. H., Choi, Y. H., Chang, Y. S., Xu, X., Kim, J. M., Kim, J. W., Jang, C. (2010). Probabilistic fracture mechanics round robin analysis of reactor pressure vessels during pressurized thermal shock. J. Nucl. Sci. Technol 47 (12): 1131-1139. doi: 10.1080/18811248.2010.9720980.

[10] Fracture Analysis of Vessels Oak Ridge FAVOR, v09.1, Computer Code: Theory and Implementation of Algorithms, Methods and Correlations, Oak Ridge National Laboratory, 2010.

[11] EPRI TR-105001. (1995). Documentation of Probabilistic Fracture Mechanics Codes Used for Reactor Pressure Vessels Subjected to Pressurized Thermal Shock Loading, Electric Power Research Institute.

[12] Huang, C. C., Chou, H. W., Chen, B. Y., Liu, R. F., Lin, H. C. (2012). Probabilistic fracture analysis for boiling water reactor pressure vessels subjected to low temperature over-pressure event. Ann. Nucl 43: 61-67. doi: 10.1016/j.anucene.2011.12.028.

[13] Park, J. S., Choi, Y. H., Jhung, M. J. (2016). Probabilistic fracture mechanics analysis of boling water reactor vessel for cool-down and low temperature over-pressurization transients. Nucl. Eng. Technol 48 (2): 543-553. doi: 10.1016/j.net.2015.11.006.

[14] The Finite-Element Method in Heat Transfer Analysis. (1996). New York: John Wiley & Sons Press.

[15] EPRI NP-719-SR. (1978). Flaw Evaluation Procedures: ASME Section XI, Electric Power Research Institute.